International Journal of Innovation and Scientific Research
ISSN 2351-8014 Vol. 26 No. 1 Aug. 2016, pp. 236-254
© 2015 Innovative Space of Scientific Research Journals
http://www.ijisr.issr-journals.org/

Temperature fluctuations at interannual and decennial timescales on the eastern mountainous region in Democratic Republic of the Congo from period of 1940 to 1997

A. Mbata Muliwavyo, J.M. Tshitenge Mbuebue, E. Phuku Phuati, F. Tondozi Keto, R.Bopili Mbotia, and Ndotoni Zana

Department of Physics,
Faculty of Sciences, University of Kinshasa,
P.O.Box 190 Kinshasa XI, DR Congo

Copyright © 2016 ISSR Journals. This is an open access article distributed under the ***Creative Commons Attribution License***, which permits unrestricted use, distribution, and reproduction in any medium, provided the original work is properly cited.

ABSTRACT: The singular spectral analysis, the multitaper method and the wavelet analysis were applied to the standardized average series of the temperatures in the oriental mountainous zone in the Democratic Republic of the Congo in order to determine the periods of temperature fluctuations at interannual and decennial timescales in that region. These different spectral methods reveal in the temperatures of this region a signal of four years period close. The spectral analysis by wavelet coherence was also applied to the couple made of temperature series and each principal characteristic indice of Atlantic, Indian and Pacific basins in order to assess the influence of these basins on temperatures over that region . This analysis shows that the phenomenon El Ninõ Southern Oscillation phenomenon and the Western Hemisphere Warm Pool are the principal drivers of the temperature fluctuations in this area on the interannual scale of 2-8 years, the coherence's peak between the temperatures and these phenomena is located at approximately four years. The anomalies of sea surface temperatures of the tropical Atlantic Ocean also contribute to the fluctuations of the temperatures in this area on a scale 2-4 years by the means of the Atlantic Multidecennial Oscillation, the variability of the Tropical Northern Atlantic and the Atlantic Meridional Mode. The contributions of the oscillation of the North Atlantic, the variability of the Tropical Southern Atlantic and the Dipolar Mode of the Indian Ocean to the fluctuations, on interannual and decennial timescales, of the temperatures on this mountainous region are not significant.

KEYWORDS: coherence, fluctuations, singular spectral analysis, multitaper method, wavelet analysis.

1 INTRODUCTION

The temperature fluctuations in the Democratic Republic of the Congo (DRC) are understudied not only for lack of reliable data and the low number of the operational weather stations on a vast territory but also because there does not exist thermal season in the tropical zone. The rare studies carried out on Central Africa concentrated on the seasonal variability of precipitations on this area where the subsistence agriculture nourishes the majority of the population. The results of certain studies of climate variability carried out in West Africa and Western part of the Congo basin are sometimes extended to the Democratic Republic of the Congo. However the Democratic Republic of the Congo has his own climatic, orographical, floristic, hydrographic facets which can modulate its temperatures. The temperature variability over DRC should be studied in order to increase the knowledge of climatology of this territory and to aid the scientific community to assess diverse scenarios of climate change in DRC. The increase in temperatures caused the reduction in the populations of fish in African lakes like the Lake Tanganyika [1]. Certain plant species can also know an extinction following a rise in temperature on a given area [2]. Certain genius works require a good knowledge of the climate and its variations over a long period of time. The variations of the temperatures are perceptible on certain areas in the Democratic Republic of the Congo as certain writings testify some [3]. Tendencies of significant increase in temperature were highlighted in all Africa [2] but this temperature variation is not due mainly to the variability of the phenomenon of Southern Oscillation El Ninõ and could be, in the Congo basin, a fruit of the human activity [3]. Over which periods and time scales these variations did proceed? Much

more some of its imperceptible variations influence also the daily life of the population and require to be studied in order to better apprehend the influence of the climate on this tropical space and to adapt to these variations.

Our study is organized as follows : after a short introduction comes the section 2 subdivided into three subsections in which we describe the study area in subsection 2.1 , we present the data in subsection 2.2 and we describe in subsection 2.3 all the methods which will be used in this article. The section 3 presents results and their discussions and in section 4, a conclusion closes this study.

2 MATERIALS AND METHODS

2.1 STUDY AREA

The territory in the Democratic Republic of the Congo (DRC) is located between 5°30' Northern latitude and 13°50' of Southern latitude, and between 12°15' and 31°15'E of longitude, a third being located at the north of equator. The entire territory in DRC is almost included in the basin of its eponym river, the Congo River, Second River of the world by its flow (38.000 m3/s on average) and the surface of its basin. Located in the intertropical convergence zone, the DRC is a country of intense convection, intense evapotranspiration and very high moisture which all lead to a strong nebulosity and a high rainfall along the year [4]. With a large part of its area covered by African wet forests, the DRC is, with Brazil and Indonesia, one of the three principal convective countries [5]. By their immense potential of carbon storage and their impact on the total cycle of water through the recycling of water and by the surface which they occupy, the DRC forests have certainly an influence on the climatic system but not clearly quantified for various reasons [4].

Contrary to West Africa, in Eastern Africa and the Southern Africa where the climatic modes were the subject of many investigations [6], central Africa- the Congo basin and particularly the RDC- is an understudied area because of the insufficiency of its infrastructures and unavailability of its climatic stations data in the international recordings [7]. The DRC is thus an area to be visited compared to its climatology and with the variability of its climatic parameters.

Dominated by an immense depression of average altitude 400 m designed as the central basin and drained by the Congo River and its tributaries, the relief of the DRC consists of plains and staged plates which connect this basin to the peripheral plateau of altitude lower than 600 m on its northern circumference [8]. The eastern edge of the DRC is consisted of mountainous chains along lakes Tanganyika, Kivu, Edouard and Albert. The southern plateau reaches more than 1000 m of altitude and with south-east; the Kundelungu mounts, in the west of the lake Moero, culminate to 1600 m of altitude [8]. In the west, the circumference of the central basin reaches 1000 m of altitude on the Cristal mounts where the Congo River dug a narrow passage in order to reach the Atlantic Ocean while passing by a narrow coastal plain formed by its estuary and the deposited alluvial grounds [8].

In DRC, according to Köppen-Geiger classification, the equatorial zone counts successively Af and Am zones covered by the immense equatorial forest [9]. After this forest we meet savanna covering the outlying highlands of the Congo basin. As one moves away from the equator towards the north or the south, after the area Am one meets then the peripheral highlands with Aw_n type climate where n (n= 1, 2, …, 6) is the number of months of dry season: wooded savanna areas corresponding to the zones $Aw_2 - Aw_4$ with opened forests, or grassy savanna areas corresponding to the zones $Aw_5 - Aw_6$ with dry forests cover these lands [10]. A heterogeneous vegetation whose floristic composition depends on altitude covers the eastern mountains in DRC: mountain forests and forests of bamboos in the Cf zones, savannas of highlands or dry forests of the highlands in the Cw zones [10], [11], [12].

The interest zone in this article corresponds to the eastern mountainous region in the DRC. Located at the west of the Valley Rift, between 2°45' of southern latitude and 2°30' of Northern latitude, this area is a narrow band made up of mountainous chains, being able to reach 3000 m of altitude, and volcanoes [11]. Its climate is a mountain climate. According to the Köppen classification, it is of Cf type between 1200 and 1900 m of altitude and Cw type beyond approximately 1900 m [11]. The weather stations of this study area are represented on figure 1, their geographical coordinates are consigned in table 1.

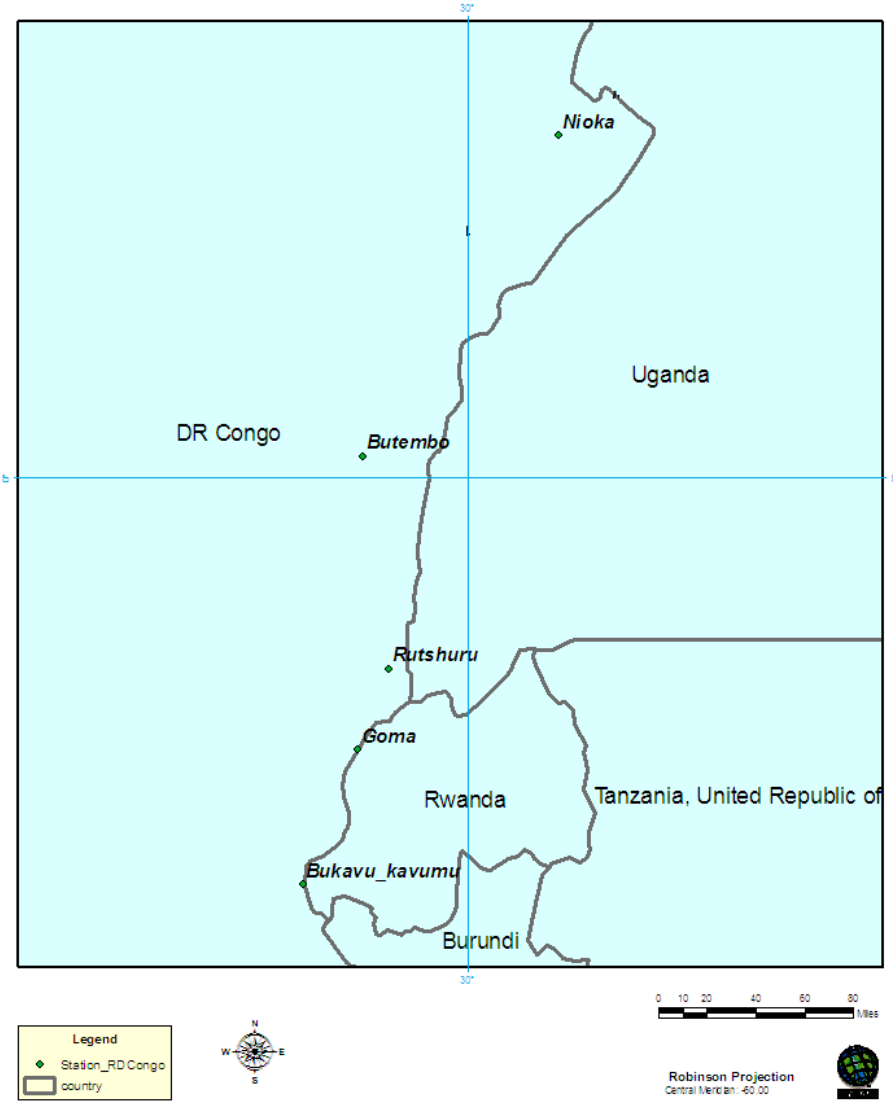

Fig. 1. Weather stations of study zone. These stations are located near the eastern frontiers of the DRC

Table 1. Geographical coordinates of the zone of study. All the study zone stations are located in a small band

Stations	Latitude	Longitude
Butembo	0°08'N	29°17'E
Goma	1°44'S	29°12'E
Kavumu	2°18'S	28°48'E
Nioka	2°08'N	30°37'E
Rutshuru	1°11'S	29°26'E

2.2 DATA

The lack of stations meteorological data for the DRC pushed us to turn us towards the data of "Climatic Research Unit" (CRU). Moreover, the data of the climatic indices which will be used are downloaded from the site of the NOAA: http://www.esrl.noaa.gov/psd/data/climateindices/list/, except the dipole mode index who is downloaded from the site: http://www.jamstec.go.jp/frcgc/research/d1/iod/DATA/dmi.monthly.txt.

In order to determine the possible links between the temperatures fluctuations of our study area and the regional or remote climatic phenomena, we resort to certain climatic indices relating to the oscillations of the sea surface temperatures

of the Atlantic, Indian and Pacific Oceans and with two indices related to atmospheric circulation. These various climatic indices which will be analyzed conjointly with the standardized time series of temperatures on the eastern mountainous area in the Democratic Republic of the Congo are:

- the index of the Atlantic Multidecadal Oscillation [13],
- the index of the variability of the Tropical North Atlantic (TNA)[14],
- the index of the variability of the Tropical South Atlantic (TSA)[14],
- the index of the Atlantic Meridional Mode (AMM) [15]
- the index of the North Atlantic Oscillation (NAO) [16], [17]
- the index of the dipole of the Indian Ocean or the Dipole Mode Index (DMI) [18],
- the southern oscillation index (SOI)[19],
- the Nino 3.4 index[20],
- the Trans Nino index (TNI)[21],
- the index of the Western Hemisphere Warm Pool (WHWP) [22].

The definition of each different index is given in reference listed after the considered index.

The temperature fields used in this article are extracted from the CRU 3.10 gridded database on the globe except the polar regions with a resolution of 0.5 ° x 0.5 °; they are a set of monthly data showing the evolution of temperatures over the period 1901-2009. The database is built from more than 4,000 weather stations distributed over the land where the missing data are estimated using 1961-1990 reference period according to the interpolation and homogenization methods [23].

A hierarchical classification on principal component analysis is applied to the temperature data of the weather stations of the DRC extracted the CRU database. The weather stations are thus grouped and each group constitutes a study zone. The average series for each group is calculated and then standardized. This procedure consists in eliminating the annual cycle from the data and dividing the anomalies thus obtained by the standard deviation. The temperature time series used for investigation in this article is thus a time series of reduced monthly anomalies of the temperatures. The weather stations of the study zone extracted from the CRU database are represented on figure 1.

The temperatures in this study area follow on a seasonal scale a unimodal mode with lower temperatures at July as figure 2 attests it. The time series representing the evolution of temperatures in the study zone is represented on figure 3.

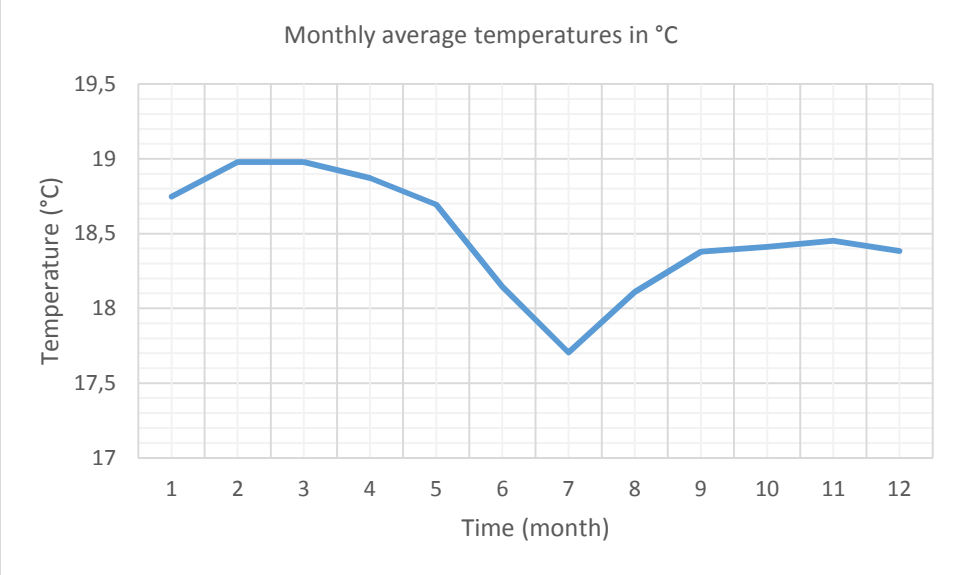

Fig. 2. Temporal seasonal evolution of the temperatures on the eastern mountainous region of the DRC. The thermal amplitude is low, the coldest month is July.

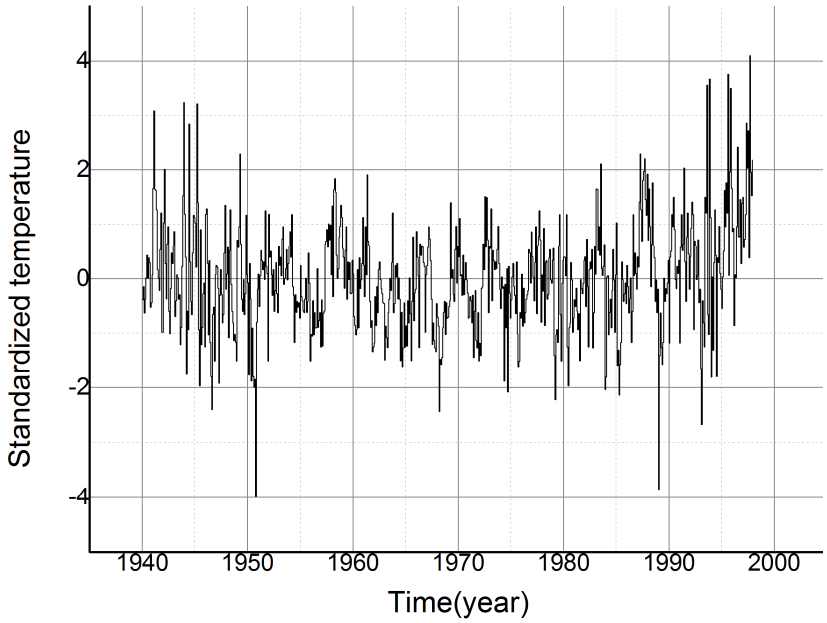

Fig. 3. Evolution of temperature anomalies over DRC eastern mountainous zone as function of time. Perceptible positive temperature anomalies, on the periods 1940-1950 and 1990-1997, denote a temperature increase while negative temperature anomalies indicate a temperature decrease.

2.3 METHODS

In order to determine periodic structures in our standardized time series of temperatures over the eastern mountainous region in the DRC, we will use two sophisticated spectral methods, the multitaper method (MTM) and the singular spectral analysis (SSA), all implemented in the SSA-MTM toolkit that can be downloaded from http://www.atmos.ucla.edu/tcd/ssa/ and the wavelet analysis. Wavelet analysis will also be used for further investigations. The code of Grinsted et al., derived from the popular Matlab code of Torrence and Compo, downloaded from http://www.pol.ac.uk/home/research/waveletcoherence/, will also be applied. The popular Matlab code of Torrence and Compo is available at http://paos.colorado.edu/research/wavelets/

2.3.1 THE MULTITAPER METHOD

Developed by Thomson [24], the "multitaper" method (MTM) is a non-parametric method of spectral analysis which allows the spectral evaluation [24], [25] by reducing the spectral leakage and provides a statistical test for the validity of the spectral peaks and their amplitudes [26] and the signal reconstruction [27] of a time series whose spectrum is formed of the continuous and singular components. This method, "which uses multiple orthogonal tapers to describe phase and amplitude modulated structures" [28] embedded in a univariate time series, was largely applied to the signals in various fields [29]. Combined with the Mann-Lees test [30], it makes possible to isolate independently the background noise, the harmonic signals and the narrow band anharmonic signals present in the spectrum of a time series [31].

For a time series data $X(t)$, $t = 1, \dots, N$, the MTM determines K uncorrelated estimates of the periodogram from orthogonal tapers, called Slepian tapers $w_k(t)$, $k = 1, 2, \dots, K$ well selected, which provide an optimal resolution and minimize the spectral leakage. The K tapered Fourier transforms are given by the equation:

$$Y_k(f) = \sum_{t=1}^{N} w_k(t) X(t) e^{i2\pi f t \Delta t}$$

The optimal windows $w_k(t)$ are eigenvectors obtained from $N \times N$ eigenvalue problem:

$$A w_k = \lambda_k w_k$$

where λ_k, the eigenvalue associated with the eigenvector w_k, measures resistance to the spectral leakage of the window and the matrix A has with the form

$$A_{mn} = 2\Delta t W sin(2\pi W(n-m)\Delta t)$$

With Δt the interval of sampling, $W = pf_R$ the resolution in frequency of the spectral estimate, $f_R = (N\Delta t)^{-1}$ the Rayleigh frequency of the time series and p a suitably selected entire. The eigentapers with $\lambda_k \sim 1$ can be used to construct spectral estimates resistant to the spectral leakage.

"Only $K = 2p - 1$ tapers are usefully resistant to the spectral leakage" [28], [31].

From K spectral estimates, one obtains, after adjustment of the relative weights on the contributions of each one of K eigenspectra, a spectral estimate resistant to the leakage, called adaptively weighted multitaper spectrum by the relation

$$P_X(f) = \frac{\sum_{k=1}^{K} b_k^2(f)\lambda_k |Y_k(f)|^2}{\sum_{k=1}^{K} b_k^2(f)\lambda_k}$$

Where $b_k(f)$ is a " data – adaptively determined weighting function" of the eigenspectra which seeks to minimize a broad-band leakage for a nonwhite but locally white process [28], [31].

Only the spectral fluctuations at frequencies higher than f_R can be resolved, the spectrum resolution frequency is equal to $2pf_R$.

2.3.2 SINGULAR SPECTRAL ANALYSIS

Designed to extract information from the short and noisy time series without preliminary knowledge of dynamics at the origin of the time series, the singular spectral analysis (SSA) is a non-parametric method which uses an adaptive data set and thus provides an outline on the dynamics of the system which generated this series. Using anharmonic basis functions derived from the lagged covariances of the data series, it can identify the recurring modes in time and isolate the periodic components and the tendencies from a time series [28].

The singular spectral analysis proceeds by three basic stages [32]:

i. the embedding of the sampled time series $\{X(t) : t = 1, \ldots, N\}$ in a vector space of dimension M, in other words the representation of the behavior of the system by a succession of sights of the series overlapping through a slipping window of M points ,

ii. the calculation of the $M \times M$ data covariance matrix C_D ; and

iii. the diagonalisation of matrix C_D.

The time series $\{X(t) : t = 1, \ldots, N\}$ is embedded in a vector space of dimension M by considering the M shifted copies $\{X(t-j) : j = 1, \ldots, M\}$. The choice of dimension M is not obvious, but the analysis of the periods by SSA is efficient in the range $\left(\frac{M}{5}, M\right), M = N/3$ [33].

Three different algorithms allow us to compute covariance matrix C_D

In the Broomhead-King algorithm, a window length M is moved along the time series, producing a sequence of $N' = N - M + 1$ vectors in the embedding space. This sequence is employed to obtain the trajectory matrix, D, of dimension $N' \times M$, where the kth line is the kth view of the time series through the window. D can also be looked as made up of its column vectors $X^{(m)}$, each one of length M, i.e.

$$D \equiv \left[X^{(1)} \middle| X^{(2)} \middle| \middle| X^{(3)} \middle| \ldots \middle| X^{(N-M+1)} \middle|\right]$$

In this approach, the covariance matrix C_D is defined by

$$C_D = \frac{1}{N'} D D^T$$

whose elements are obtained from the relation [29]

$$c_{ij} = \frac{1}{N-M+1} \sum_{t=1}^{N-M+1} X(i+t-1)X(j+t-1)$$

The Vautard-Ghil algorithm consists of the matrix C_D estimate from the data as a Toeplitz matrix whose entries c_{ij} are given by the relation [31]:

$$c_{ij} = \frac{1}{N-|i-j|} \sum_{t=1}^{N-|i-j|} X(t)X(t+|i-j|)$$

The Burg covariance matrix is obtained from an iterative process based on an autoregressive model having a number of autoregressive coefficients equal to the length of SSA window.

The square roots $\{\sqrt{\lambda_k}, k = 1,\ldots,M\}$ of the eigenvalues λ_k of the covariance matrix ranged by decreasing order are the singular values whose the corresponding set constitutes the singular spectrum [31]. Each eigenvalue gives the variance of the time series in the direction specified by the corresponding eigenvector E_k , called temporal empirical orthogonal function (T-EOF). The scree plot of the singular values gives two areas: the first, of steep slope, represents the signal, and the second constituting a "more or less flat floor" represents the noise. The k-th temporal principal component (T-PC) A_k is the projection of the data set on the eigenvector E_k and is thus defined by the relation:

$A_k(t) = \sum_{j=1}^{M} X(t+j-1)E_k(j),\ t = 1,\ldots,N-M+1$

for each EOF E_k of components $\{E_k(j) : j = 1,\ldots,M\}$

In order to distinguish the significant signal from the noise or the background, the null hypothesis of red noise is used. The SSA method combined with the test which compares the statistics of a red noise simulated time series with that of a given climatic time series is called Monte Carlo SSA method.

The Monte Carlo version of SSA [34] allows to separate the quasi-regular oscillations and the nonlinear tendencies from a time series, to detect the phase and amplitude modulated oscillations, to follow through the reconstructed components the amplitude variations, the phase and the frequency associated with the almost broad spectral peaks. The pairs of oscillations in phase quadrature identified by this method can represent an anharmonic nonlinear oscillation [33].

2.3.3 WAVELET ANALYSES

Most of climatic time series are no stationary and Fourier analysis is inappropriate to the study of such series. Wavelet analysis is used in this case to decompose a time series into frequency and time components and the dominant modes of variability and transitory aspects can therefore be extracted [35]. The analysis of the intermittent localized oscillations present in a signal and their temporal localization can thus be studied.

In the place of the functions sine and cosine used in the Fourier transform, the continuous wavelet analysis uses a wavelet function $\psi(t)$ which is a function of finite energy:

$\int_{-\infty}^{+\infty} |\psi|^2 dt = 1$

and

a function of zero mean, i.e the wavelet must be an oscillating function

$\int_{-\infty}^{+\infty} \psi(t)\, dt = 0$

Moreover, $\psi(t)$ is often required to have a certain number of vanishing moments:

$\int_{-\infty}^{+\infty} t^k \psi(t) dt = 0$ with $k = 0,1,2,\ldots$

This property improves the efficiency of $\psi(t)$ in the detection of singularities in the signal. Indeed, the wavelet becomes blind to polynomials of degree inferior or equal to k which constitute the smoothest part of the signal.

Several types of wavelet functions (Haar, Mexican hat, Morlet, Paul …) with the specific properties and adapted to the various analyses exist [36]. The Morlet wavelet, defined as a complex exponential wave damped by a Gaussian envelope of equation [35], [36]:

$$\psi_0(\eta) = \pi^{-1/4} e^{i\omega_0\eta} e^{-\eta^2/2}$$

where ω_0 is an adimensional frequency often taken equal to 6 in several analyses and $\eta = st$, s the wavelet scale [37], is frequently used in continuous wavelet analysis and will be used in this article.

The continuous wavelet transform is applied as a bandpass filter. The wavelet is stretched in time by varying its scale s and by normalizing it to have an energy equal one.

As a passband filter applied to the time series, the continuous wavelet transform of a discrete time series $(X_n, n = 1,2,\dots,N)$ with a uniform temporal step δt is defined by the convolution of X_n with the shifted and standardized wavelet. It is given by the relation

$$W_n^X(s) = \sqrt{\frac{\delta t}{s}} \sum_{n'=1}^{N} X_{n'} \psi_0 \left[(n' - n) \frac{\delta t}{s} \right]$$

The local wavelet power spectrum of a time series at the scale s and the time index n is given by $|W_n^X(s)|^2$. It allows us to describe the temporal intermittent oscillations present in a time series. The periodicities present in a signal, the peaks and the fluctuations or energy bands recovering certain scales of time can be observed on the local wavelet power spectrum of a time series.

The time-averaged wavelet power spectrum, also called global wavelet power spectrum, $S(s)$, and defined by the relation:

$$WGS(s) = \sum_n |W_n^X(s)|^2$$

provides a unbiased and consistent estimate of true power spectrum of a time series and can therefore be used for identification of periods of intermittent oscillations embedded in a signal [36].

The power fluctuations on a range of scales can be examined through the wavelet power spectrum weighted in scale. This last is defined as the weighted sum of the wavelet power spectrum between the scales s_1 and s_2 by the expression [36]:

$$\bar{W}_n{}^2 = \frac{\delta j \delta t}{C_\delta} \sum_{j=j_1}^{j_2} \frac{\left|W_n(s_j)\right|^2}{s_j}$$

where C_δ, an independent factor and constant for each wavelet function, is equal to 0,776 for the Morlet wavelet and δj the scale step. The variance of a time series is thus obtained as a function of time.

As the wavelet is not completely localized in time, the continuous wavelet transform has edge artifacts and a cone of influence is then introduced in order to take into account edge effects [36], [37], [38].

The quantification of the possible links between two nonstationary signals identified by their time series X and Y, between the modes of variability detected and the physical mechanisms at the beginning of these modes is possible by using the wavelet coherence. As a coefficient of correlation localized in space time-frequency, the wavelet coherence, $R_n^2(s)$, is defined as the standardized cross spectrum by the spectrum of each signal [38], [39], [40]:

$$R_n^2(s) = \frac{|\langle s^{-1} W_n^{XY}(s) \rangle|^2}{\langle s^{-1} |W_n^X(s)|^2 \rangle \langle s^{-1} |W_n^Y(s)|^2 \rangle}$$

where

$$W_n^{XY}(s) = W_n^X(s).W_n^Y(s)^*$$

$W_n^Y(s)^*$ indicates the conjugated of $W_n^Y(s)$, the factor s^{-1} is used to convert with an energy unit and $\langle \ \rangle$ appoints an operator $\mathcal{L}$ of smoothing at the same time in time and scale. The operator of smoothing $\mathcal{L}$ can be written [38]:

$$\mathcal{L}(W) = \mathcal{L}_{scale}(\mathcal{L}_{time}(W_n(s)))$$

$\mathcal{L}_{scale}$ indicates smoothing along the axis of scale and $\mathcal{L}_{time}$ smoothing in time.

For the Morlet wavelet, the operator of smoothing in time and the operator of smoothing in scale are given respectively by [38]:

$$\mathcal{L}_{time}(W)|_s = \left(W_n(s).c_1 e^{-\frac{t^2}{2s^2}} \right)\Big|_s$$

$$\mathcal{L}_{scale}(W)|_n = (W_n(s).c_2 \Pi(0{,}6s))|_n$$

where c_1 and c_2 are constants of standardization and Π is the rectangular function of width δj_0, the length of decorrelation of the scale. δj_0=0.60 for the Morlet wavelet [37]. R_n^2 is limited between 0 and 1.

The wavelet coherence analysis makes possible to characterize the degree of linearity between two processes for all localizations time-scale [37], [38].

The difference in phase $\phi_n(s)$ of the wavelet coherence is given by

$$\phi_n(s) = arctg\left(\frac{\Im\{\langle s^{-1}W_n^{XY}(s)\rangle\}}{\Re\{\langle s^{-1}W_n^{XY}(s)\rangle\}}\right)$$

Coherence phase between two series is seen in the wavelet coherence spectrum as arrows indicating dephasing between the two phenomena or the delay between two signals [37], [39]: horizontal arrows pointing towards the right for two phenomena in phase, horizontal arrows pointing towards the left for two phenomena in opposition of phase and vertical arrows for two phenomena with a nonlinear relation. In all the cases, the horizontal arrows stand for a linear relation between the phenomena considered. The time and frequency intervals where the two phenomena have a strong interaction can thus be highlighted by the wavelet coherence [39].

The scale-averaged wavelet coherence spectrum, defined in the same manner that the scale-averaged wavelet spectrum of a time series, enables us to follow the temporal evolution of coherence between two time series in a specific period band.

The global wavelet coherence spectrum, GWCS (S), is defined by [39]:

$$GWCS(s) = \sum_n R_n^2(s) = \sum_n \frac{|\langle s^{-1}W_n^{XY}(s)\rangle|^2}{\langle s^{-1}|W_n^X(s)|^2\rangle\langle s^{-1}|W_n^Y(s)|^2\rangle}$$

and allows us to identify the periods of strong coherence between two time series.

False positive results can also be obtained by wavelet analysis since random fluctuations can produce high values of spectral power or coherence related on the underlying process and not to the time series. To mitigate this problem, one often compares the wavelet power spectrum of a temporal geophysical series with that of a theoretical red noise [36] which can be very well modeled by an first order autoregressive process; the statistical significance test proves very important. Two statistical significance tests usually used in wavelet analysis are the test of Torrence and Compo [33] extended to wavelet coherence by Grinsted et al. [37] by using the Monte Carlo methods and called “pointwise test” and the test of Maraun et al. [41] called “areawise test”. All investigation in this article is conducted at a confidence level superior or equal to 95% .

3 RESULTS AND DISCUSSIONS

3.1 FLUCTUATIONS OF THE TEMPERATURES

The periods of the signals present in the temperatures of the eastern mountainous region in RDC returned by the multitaper method of the spectral estimate are respectively (4.7 ± 0.8) years and (3.3 ± 0. 4) years (figure 4).

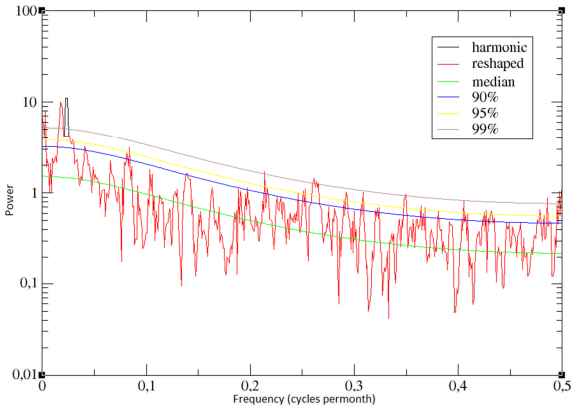

a)

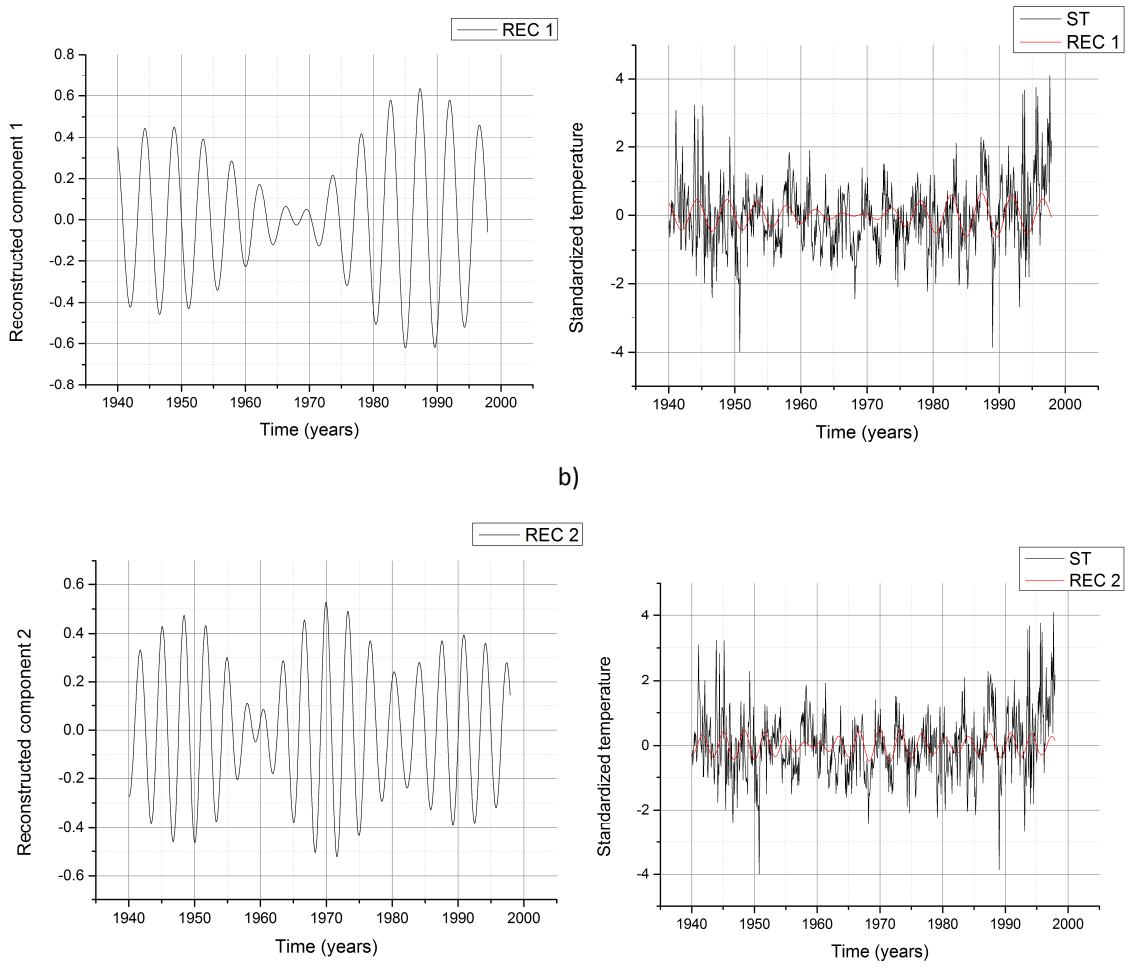

Fig. 4. MTM spectrum of the standardized temperatures (ST) in the eastern mountainous region in the DRC and reconstructed components: a) MTM spectrum of the temperatures, b) Interannual reconstructed component of period 4.7 years (REC 1 at left) and REC 1 superimposed on the original signal (at right) and c) Interannual reconstructed component of period 3.3 years (REC 2 at left) and REC 2 superimposed on the original signal (at right).

The SSA Vautard-Ghil algorithm applied to the series of the temperatures of the eastern mountainous region of the DRC reveals signals of periods (4.2 ± 0.2) and (3.3 ± 0.2) years within the temperatures of this area (figure 5).

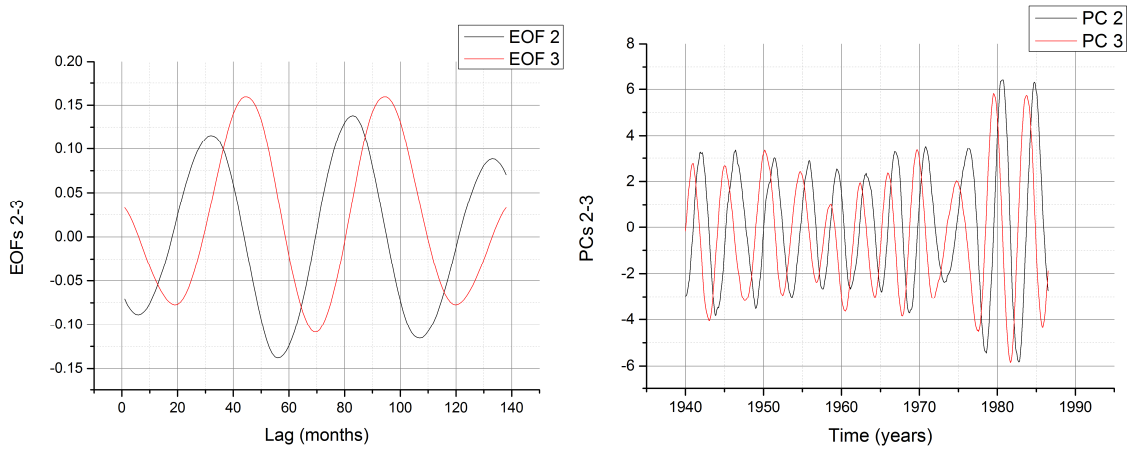

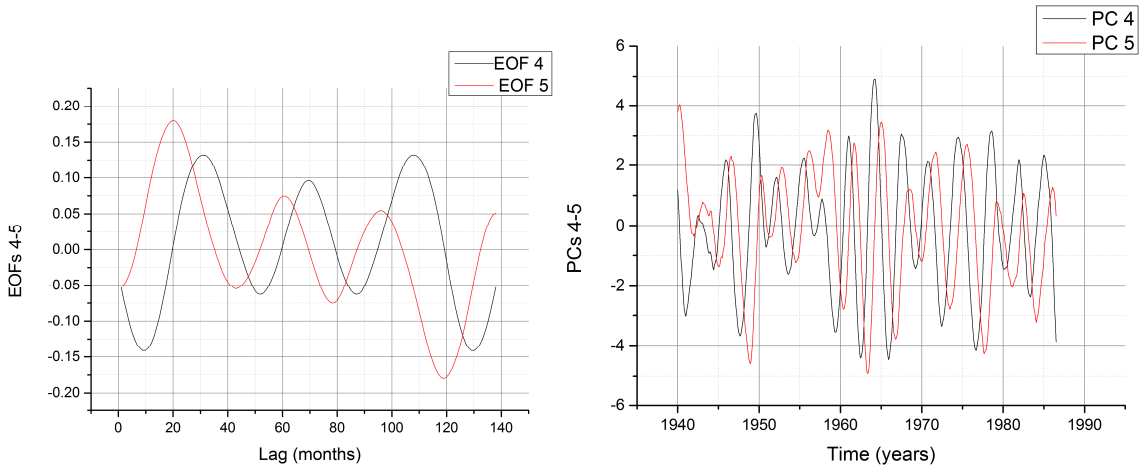

b)

Fig. 5. Empirical orthogonal functions (EOFs at left) and corresponding principal components (PCs at right) of the standardized time series of temperature in the eastern mountainous region in the DRC: a) EOFs 2 and 3 and corresponding PCs 2 and 3 b) T-EOFs 4 and 5 and corresponding PCs 4 and 5. The embedding dimension M is taken equal to 138.

Wavelet analysis of the temperatures on the same area presents to us three energy bands in the band of the periods ranging between 2 and 8 years as shown in figure 6a; the global wavelet spectrum reveals a peak at (5 ± 1) years.

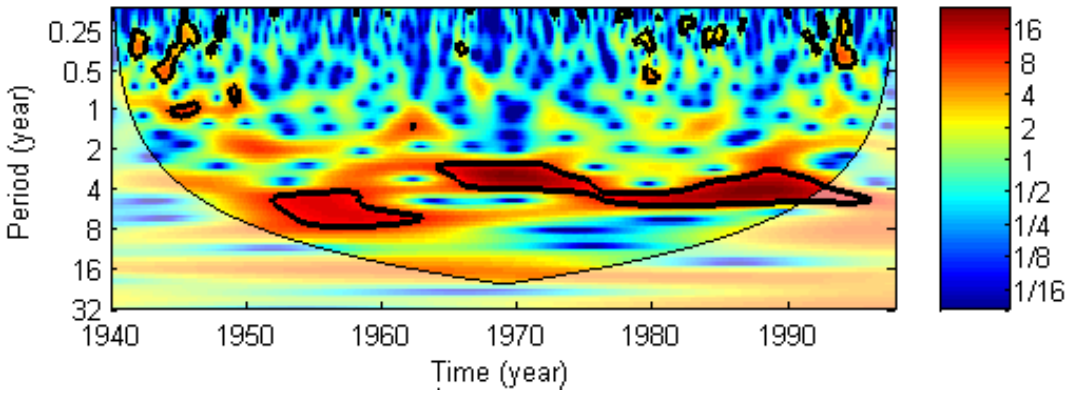

a)

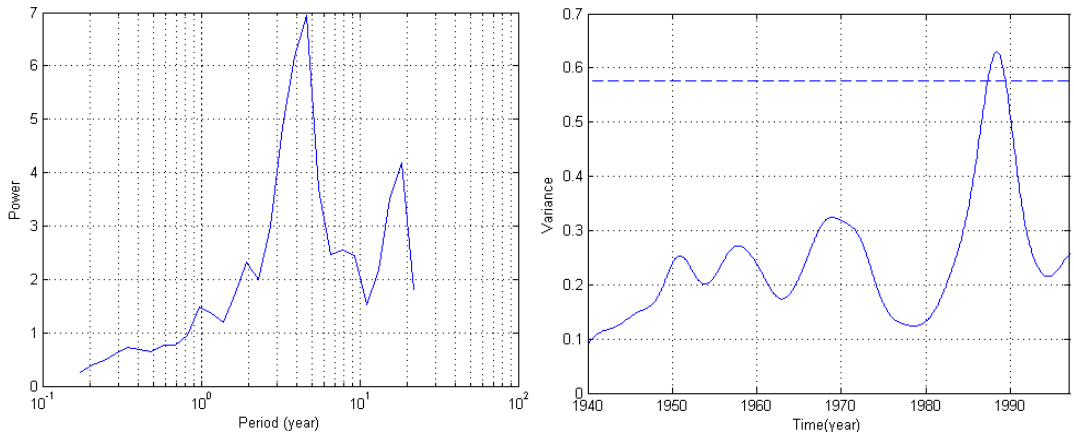

b) c)

Fig. 6. Wavelet spectra of the standardized temperatures in the eastern mountainous region in the DRC: a) local wavelet power spectrum of the temperatures, b) time-averaged wavelet power spectrum of the temperatures and c) scale-averaged wavelet power spectrum of the temperatures.

The three methods give us one common period: 4.2–4.7 years. The temperatures have peaks of variation at the following years 1952, 1958, 1969 and 1989 in the time intervals 1948-1954, 1954-1963, 1963-1979 and 1979-1994. The last peak is the most intense.

3.2 CLIMATIC FLUCTUATIONS AND INDICES OF THE ATLANTIC OCEAN

Coherence between the anomalies of sea surface temperatures of the Atlantic Ocean summarized by the following climatic indices: the AMO, the AMM, the TNA and the TSA and the temperatures on the eastern mountainous area of the DRC show a band of interaction centered over the year 1970 in the bands of 2-4 years between 1963 and 1978 roughly. This interaction, almost inexistent between the NAO, the TSA on the one hand and the temperatures on the other hand, intermittent between the AMO, the TNA, the AMM on the one hand and the temperatures on the other hand constitutes a proof that the Tropical Atlantic Ocean has a part certainly weak but significant in the temperature variability on the eastern mountainous area in the DRC.

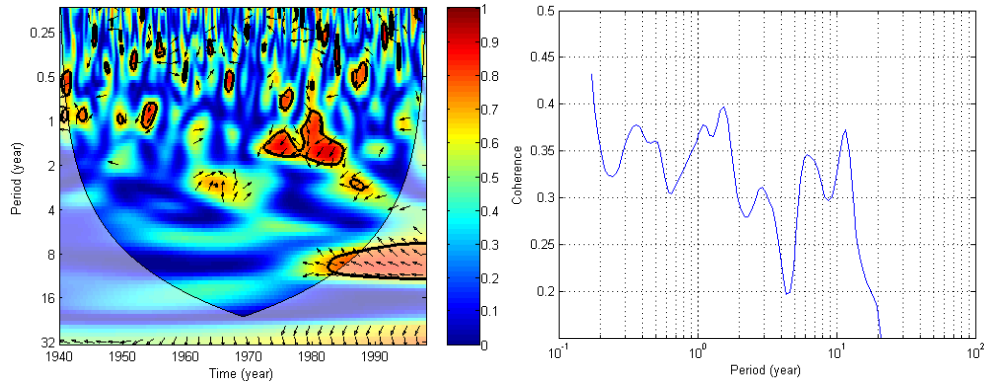

a)

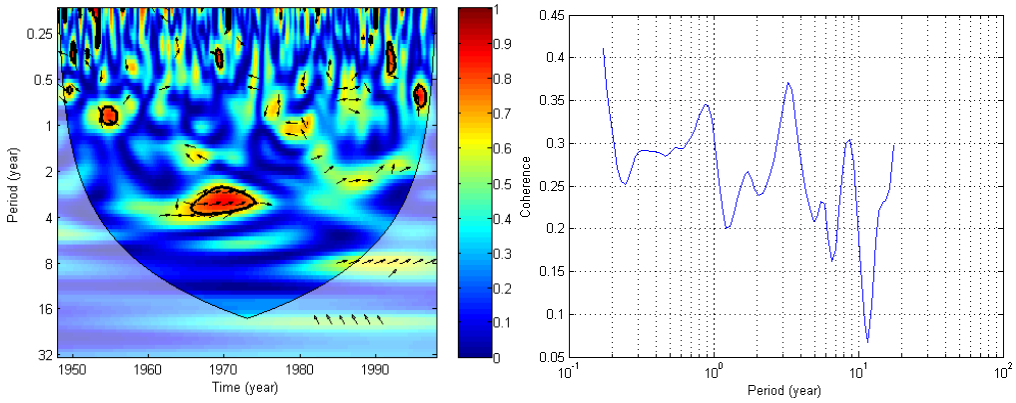

b)

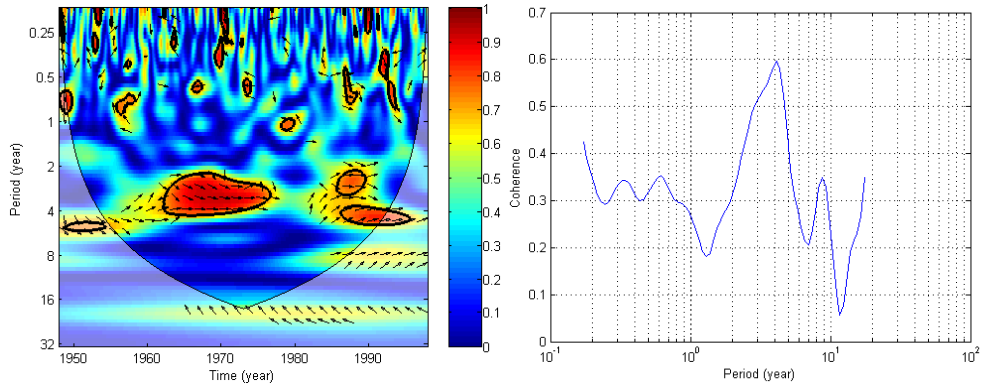

c)

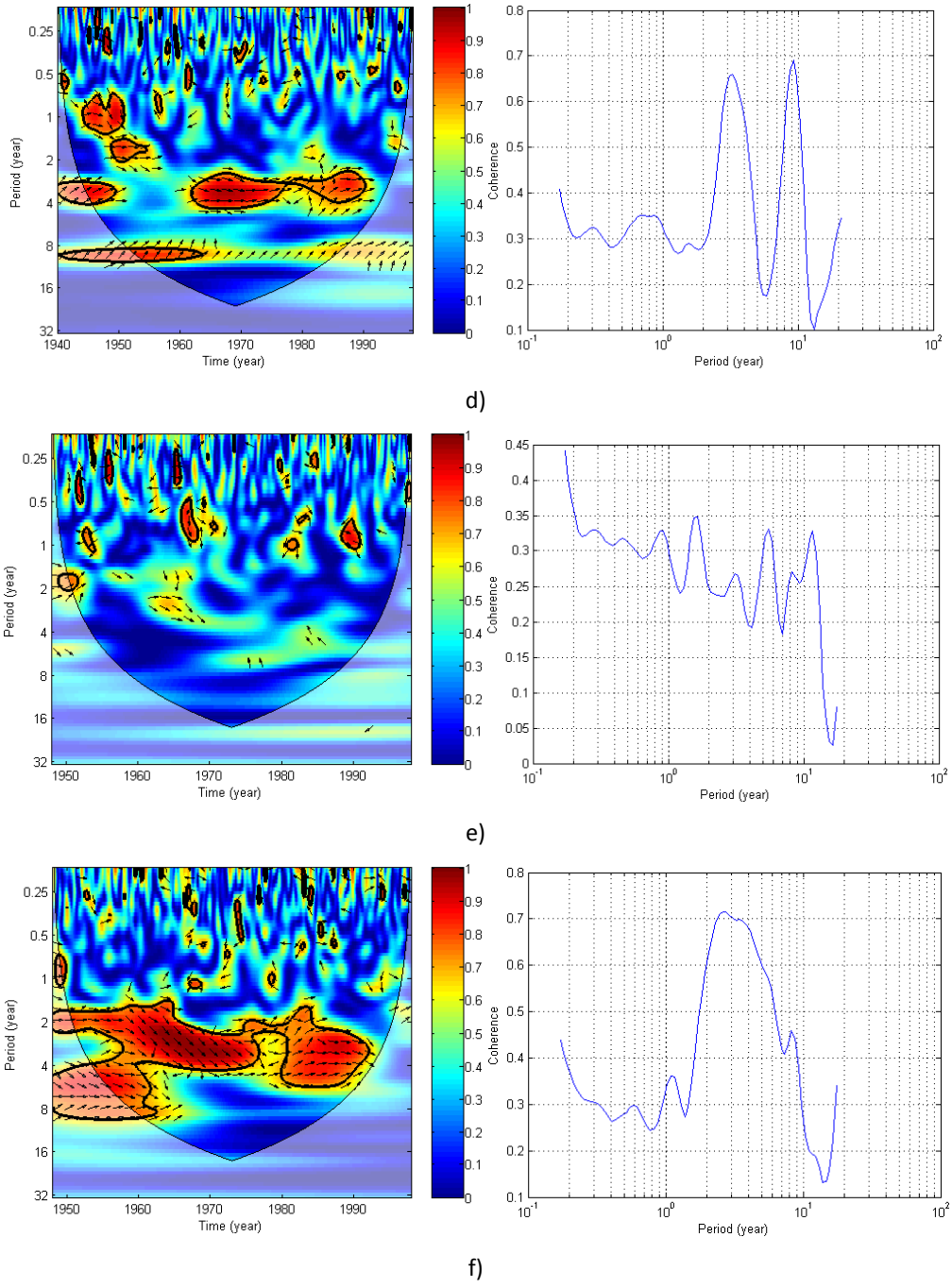

Fig. 7. Local (left) and global (right) wavelet coherence spectrum between standardized time series of temperatures on eastern mountainous region in the DRC and an indice of sea surface temperature (or sea level pressure) anomalies of Atlantic Ocean: a) NAO, b) AMM, c) TNA ,d) AMO, e) TSA et f) WHWP

The eastern mountainous sector in the DRC and the anomalies of sea surface temperatures of tropical Atlantic Ocean present a quasi-linear relationship in the 2-4 years band between 1965 and 1978. The influence of Atlantic Ocean on rainfall (climate) of the Congo Basin was underlined by Balas et al.[6], Nicholson and Dezfuli [42], Dezfuli and Nicholson [43] and Farnsworth et al.[44] at seasonal timescales but the temperature variability was not investigated.

WHWP variability in Atlantic Ocean occurs on both interannual and multidecadal timescales [45]. The years of high coherence between WHWP and temperature over eastern mountainous DRC coincide approximatively with the years of relatively high coherence between AMO, AMM, TNA and temperature over this region. According to Wang et al [45], the WHWP and the AMO have the same variability at multidecennial timescales. However, we note that at interannual and

decennial timescales, the coherence, between AMO, AMM, TNA, TSA and temperature on this region, between WHWP and temperature on this same region, varies in the same manner. At decennial time scales, no significant coherence band is observed except between the NAO and the temperature over this region after 1980. The temporal evolution of coherence between temperature over the eastern mountainous region in DRC and sea surface temperatures of tropical Atlantic Ocean is marked by the same intervals of high coherence, except for the TSA in the 1970 years which contrasts with all other indices of tropical Atlantic variability.

A low coherence is observed between temperature over this sector and these Atlantic sea surface temperature indices; this fact indicates that other climate drivers are also acting in this sector. Topography can be one of these drivers as noted by Hession and Moore [46], Oettli and Camberlin [47]. Some coherence peak years found in the wavelet coherence spectra (figure 8) coincide with some warm event years in the Tropical Atlantic sector [48].

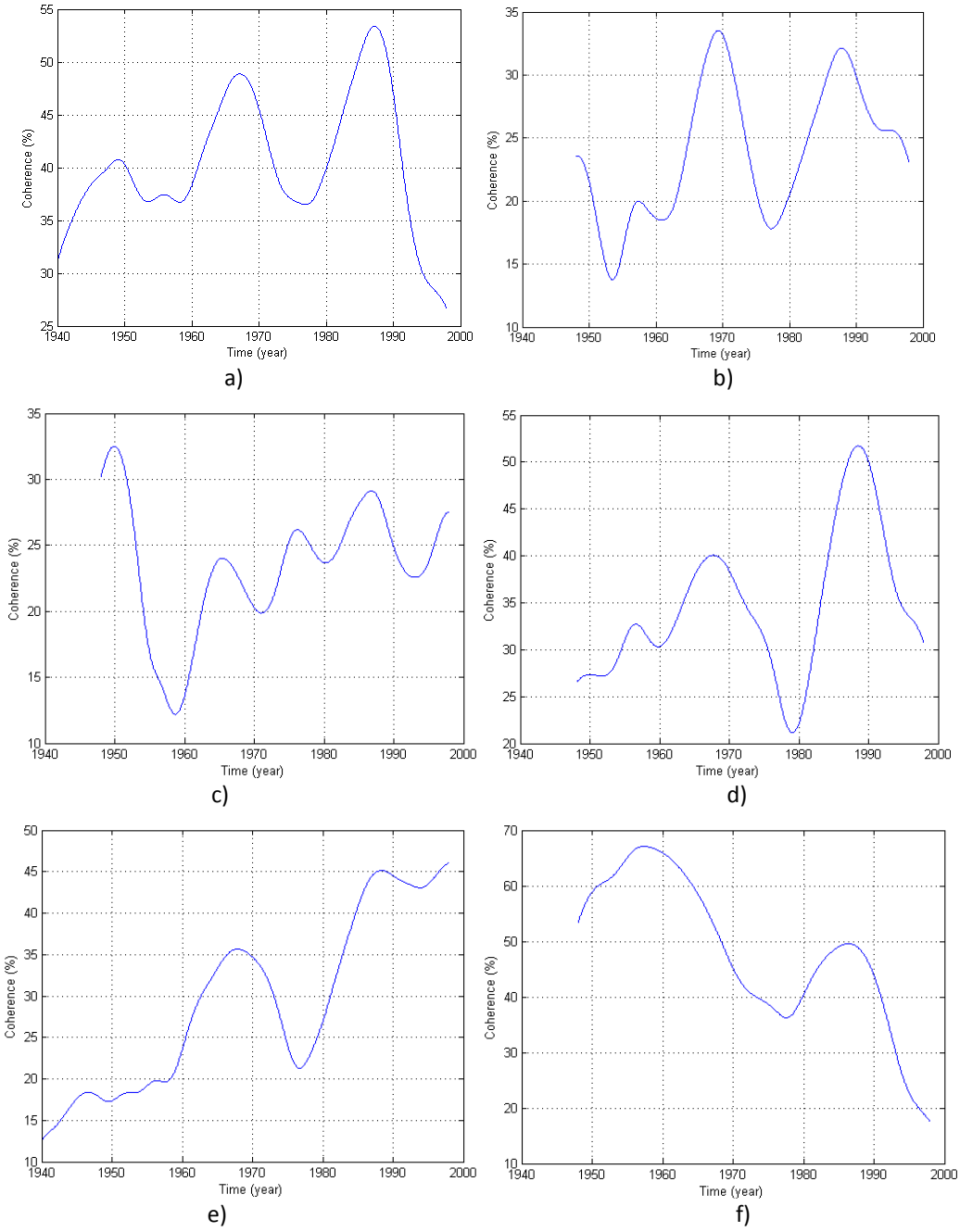

Fig. 8. Scale-averaged wavelet coherence spectrum between temperature on eastern mountainous region in the DRC and an indice of Atlantic Ocean variability : a) AMO b) AMM c) TSA d) TNA e) NAO and WHWP.

3.3 FLUCTUATIONS OF THE TEMPERATURES AND THE TROPICAL PACIFIC OCEAN

The local wavelet coherence of the temperatures with the SOI or the NINO 3.4 reveals that the temperatures in the eastern mountainous area in the DRC are almost in opposition of phase with the SOI and in phase with the Nino 3.4 in the band of the periods 2-8 years during all the study period, the coherence peaks being located roughly at 4.1 years (figure). The coherence between temperature over this region and TNI is relatively low in the band of 2-8 years. However the scale-averaged wavelet coherence spectrum between temperature and TNI reveals us most of the different years (coherence peaks) of El Nino events between 1940 and 1997(figure 9). The high mean coherence (0.5 to 0.7 approximately) between SOI or NINO 3.4 and temperature over this region during almost the study period indicates that ENSO phenomenon dominates the variability modes of the temperature fluctuations over the eastern mountainous region in the DRC at the interannual timescales.

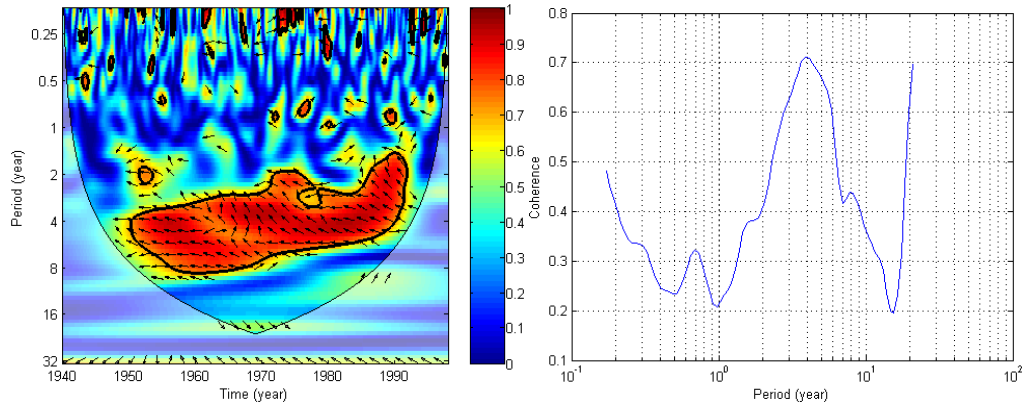

a)

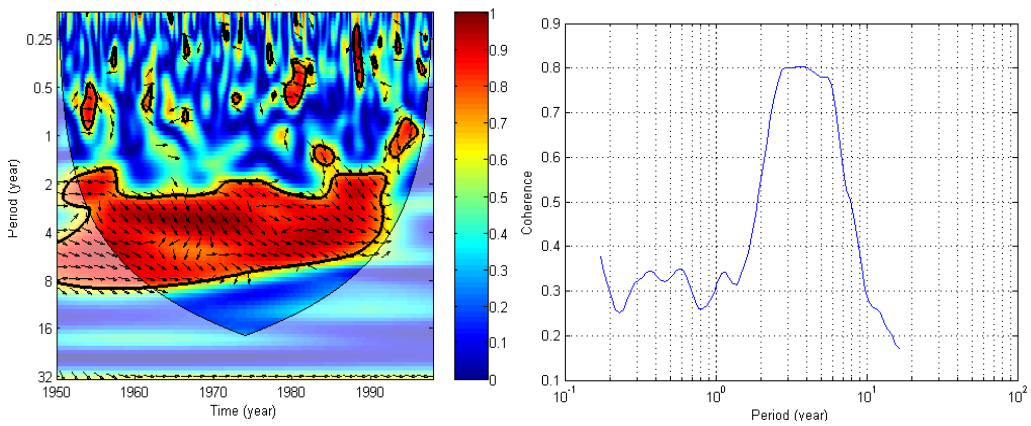

b)

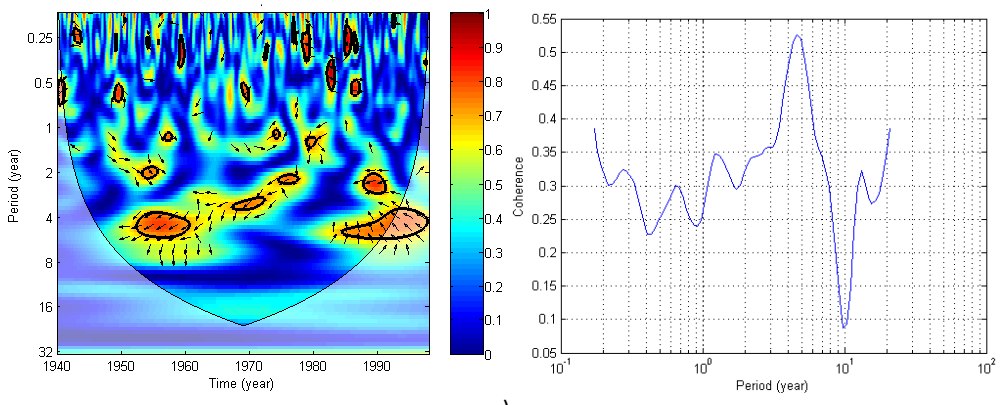

c)

Fig. 9. Local wavelet coherence and global wavelet coherence between the standardized time series of temperatures over the oriental mountainous region of DRC and: a) the SOI, b) the NINO 3.4 c) the TNI

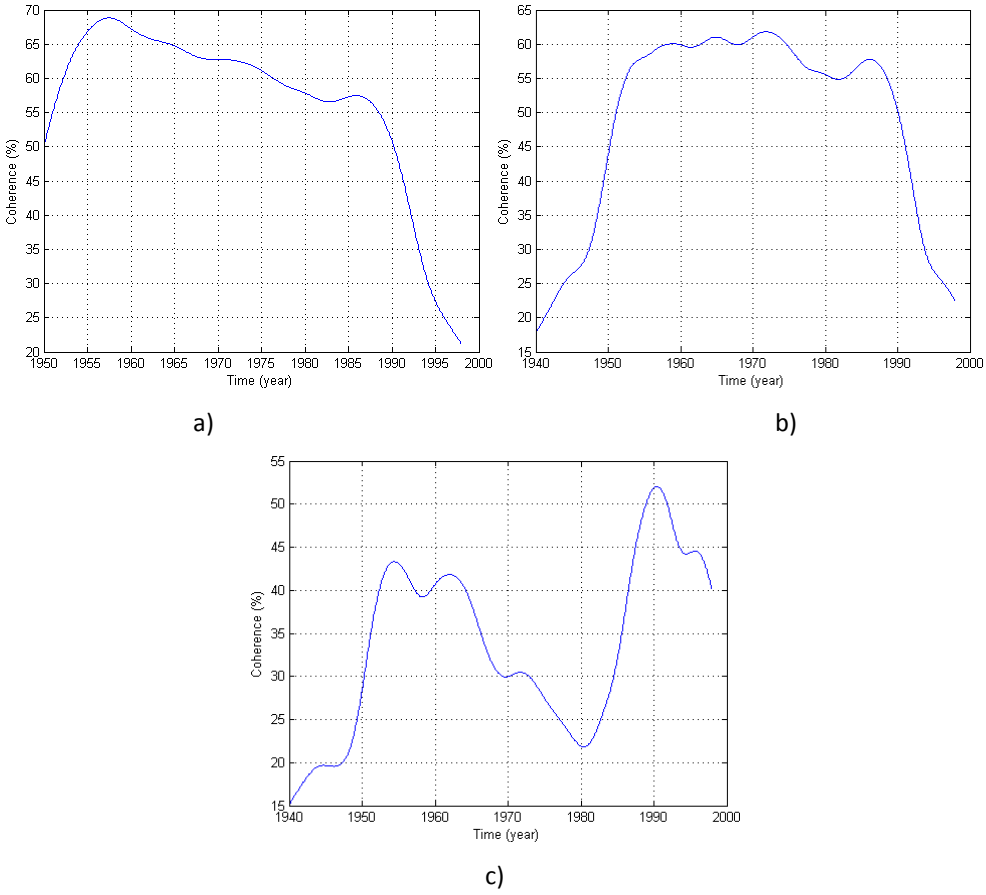

Fig. 10. Scale-averaged wavelet coherence between an ENSO indice and standardized time series of temperatures over the eastern mountainous region in the DRC: a) SOI, b) Nino 3.4 and c) TNI

3.4 INFLUENCE OF INDIAN OCEAN DIPOLE ON TEMPERATURES OVER THE EASTERN MOUNTAINOUS REGION IN THE DRC

The Indian Ocean dipole and the temperatures on eastern mountainous region in DRC present some isolated variation bands at interannual timescales. The high values of mean coherence vary between 0.38 and 0.46 at isolated years of the study period. This low coherence shows that the Indian Ocean dipole influences slightly temperature over this region.

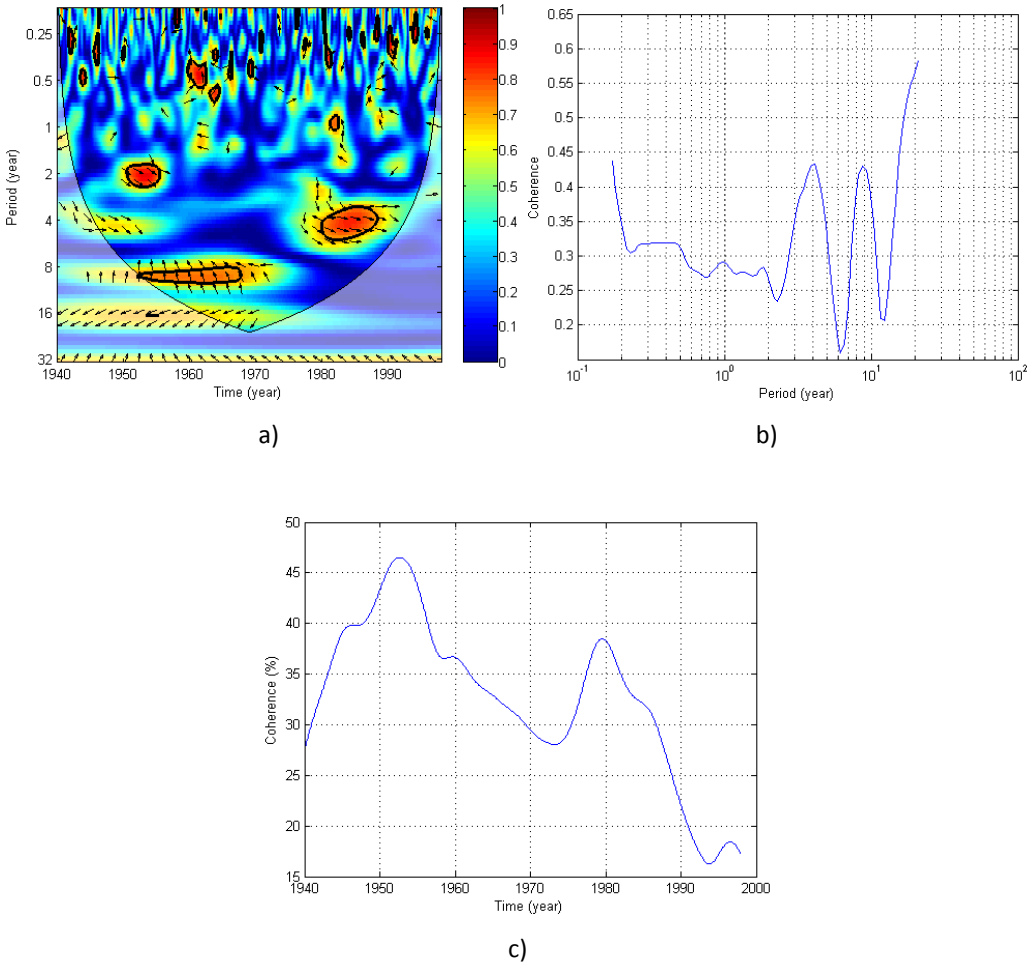

Fig. 11. Wavelet coherence analysis between the DMI and the standardized time series of temperatures over the eastern mountainous zone in the DRC: a)Local wavelet coherence , b) Global wavelet coherence c) Scale wavelet coherence

The table 2 gives the various peaks of coherence observed between the various climatic indices used in this article and the temperatures on the mountainous region. The periods of 3.1, 3.3, 8.8 and 11.7 years can be attributed to solar activity [39] but certain periods like 11.7 years are not attributed in this investigation to a significant coherence band.

Fig. 12. Coherence peaks observed between the various climatic indices and temperatures

Bands	**Bands**	**SOI**	**NINO 3.4**	**TNI**	**AMM**	**AMO**	**TNA**	**TSA**	**NAO**	**WHWP**	**DMI**
	2-4 years				3.3 yr	3.1 yr		3.1 yr		2.6 yr	
	3-6 years	4.1 yr	4.1 yr	4.6 yr			4.1 yr				4.1 yr
2-8 years	5-8 years							5.5 yr			
	8-12 years										
8-16 years	12-16 years	8.3 yr			8.8 yr	8.7 yr	11.7 yr		11.7 yr	8.3 yr	8.7 yr

4 CONCLUSION

At interannual timescales, the temperature fluctuations over the eastern mountain region in DRC are driven by the ENSO phenomenon and the WHWP. The influence of Atlantic Ocean on this region seems low but the WHWP should be one of the major drivers, with ENSO, of the interannual variability of temperature in this region. A signal of 4.1 years period which can be attributed to ENSO phenomenon, a signal of 2.6 years period relative probably to the WHWP and the high coherence between the SOI or the NINO 3.4, the WHWP and the temperature over this region attest that Tropical Pacific and Atlantic Oceans have a major impact on temperature fluctuations at interannual timescales. At decennial timescales, the solar activity

should be one of the temperature fluctuation drivers over this region. The Indian Ocean dipole has a little effect over this region.

REFERENCES

[1] Verburg, P., R. E. Kecky, and H. Kling, "Ecological consequences of a century of warming in Lake Tanganyika", Science, 301, 505–507, 2003.

[2] Collins, J. M., Temperature Variability over Africa, *J. Climate*, Vol.24, 3649–3666, 2011.

[3] Sanga N.K. and Fukuyama K., "Interannual and long-term climate variability over the Zaire River Basin during the last 30 years", *J. Geophys. Res.*, 101, 21351-21360, 1996.

[4] Haensler, A., Saeed, F. and Jacob, D. (2013): *Assessment of projected climate change signals over central Africa based on a multitude of global and regional climate projections*. In: Climate Change Scenarios for the Congo Basin. [Haensler A., Jacob D., Kabat P., Ludwig F. (eds.)]. Climate Service Center Report No. 11, Hamburg, Germany,ISSN: 2192-4058.

[5] Washington R., James R., Pearce H., Pokam W. M. and Moufouma-Okia W., "Congo Basin rainfall climatology: Can we believe the climate models?" *Philos Trans R Soc Lond B Biol Sci.* 368(1625): 20120296, 2013.

[6] Balas N., Nicholson S. E., Klotter D., "The relationship of rainfall variability in west Central Africa to sea-surface temperature fluctuations", *Int. J. Climatol.*, 1349, 1335–1349, 2007.

[7] E. Aguilar, A. Aziz Barry, M. Brunet, L. Ekang, A. Fernandes, M. Massoukina, J. Mbah, A. Mhanda, D. J. do Nascimento, T. C. Peterson, O. Thamba Umba, M. Tomou, and X. Zhang, "Changes in temperature and precipitation extremes in western central Africa, Guinea Conakry, and Zimbabwe, 1955–2006", *Journal of Geophysical Research*, Vol. 114, 2009

[8] Jules Gérard-Libois, Henri Nicolaï, Patrick Quantin, Universalis, Benoît Verhaegen, Crawford Young, «*République Démocratique Du Congo*», Encyclopædia Universalis [en ligne], consulté le 15 mars 2016. URL : http://www.universalis.fr/encyclopedie/republique-democratique-du-congo/

[9] Alain Foucault, *Climatologie et Paléoclimatologie*, Dunod, Paris, 323 pp., 2009.

[10] Sanga N. K. and Fukuyama K., "Interannual and long-term climate variability over the Zaire River Basin during the last 30 years", *J. Geophys. Res.*, 101, 21351-21360, 1996.

[11] www.wzd.cz/zoo/AF/CD/unknown/files/planed_provincial_biodiversiti_actions_99.pdf. Plans d'action provinciaux de la biodiversité, consulté le 18/06/2016

[12] Stratégie et plan d'action nationaux de la biodiversité (2015-2020) Draft 03 Septembre 2015, http://cd.chm-cbd.net/implementation/le-changement-climatique-en-republique-democratique-du-congo/strategie-et-plan-d-action-nationaux-de-la-biodiversite-2015-2020/download/fr/, consulté le 18/06/2016

[13] Enfield, D.B., A. M. Mestas-Nunez and P.J. Trimble, "The Atlantic multidecadal oscillation and it's relation to rainfall and river flows in the continental U.S.", *Geophysical Research Letters*, Vol. 28, 2077-2080, 2001.

[14] Enfield, D.B., A.M. Mestas, D.A. Mayer, and L. Cid-Serrano, "How ubiquitous is the dipole relationship in tropical Atlantic sea surface temperatures?" *JGR-O*, 104, 7841-7848, 1999.

[15] Chiang J. C. H. and D. J. Vimont: "Analagous meridional modes of atmosphere-ocean variability in the tropical Pacific and tropical Atlantic", *J. Climate*, 17(21), 4143-4158, 2004.

[16] Hurrell J.W., "Decadal trends in the North Atlantic Oscillation and relationships to regional temperature and precipitation". *Science* 269, 676-679, 1995.

[17] Jones P.D., Johnson T. and Wheeler D., "Extension to the North Atlantic Oscillation using early instrumental pressure observations from Gibraltar and South-West Iceland", *Int. J. Climatol*. 17, 1433-1450, 1997.

[18] N. H. Saji, B. N. Goswami, P. N. Vinayachandran and T. Yamagata, "A dipole mode in the tropical Indian Ocean", *Nature*, Vol. 401, 23, 1999.

[19] Philander S. G. H., *El Niño, La Niña and the Southern Oscillation*, Academic Press, San Diego, Calif., 293 pp., 1990.

[20] Trenberth K. E., "The Definition of El Niño", *Bulletin of the American Meteorological Society*, 78(12), 2771-2777, 1997.

[21] Trenberth K. E. and Stepaniak D. P., "Indices of El Niño Evolution", J. Climate, Vol. 14, 1697-1701, 2001

[22] Wang C. and D.B. Enfield, "The tropical Western Hemisphere warm pool", *Geophys. Res. Lett.*, 28, 1635-1638, 2001.

[23] Mitchell T. D. and Jones P. D., "An improved method of constructing a database of monthly climate observations and associated high-resolution grids", International Journal of Climatology, *Wiley Online Library*, 25, 693-712, 2005.

[24] Thomson, D. J., "Spectrum estimation and harmonic analysis", *Proc. IEEE*, 70, 1055–1096, 1982.

[25] Percival, D. B., and A. T. Walden, *Spectral Analysis for Physical Applications*, Cambridge Univ. Press, New York, 583 pp., 1993.

[26] Park, J., C. R. Lindberg, and F. L. I. Vernon, "Multitaper spectral analysis of high-frequency seismograms", *J. Geophys. Res.*, 92, 12,675–12,684, 1987.

[27] Ghil, M., and C. Taricco, Advanced spectral analysis methods, in Past and Present Variability of the Solar-Terrestrial System: Measurement, Data Analysis and Theoretical Models, edited by G. C. Castagnoli and A. Provenzale, pp. 137–159, *Soc.Ital. Di Fis.*, Bologna, Italy, 1997.

[28] Mann M. E. and Park J., Oscillatory spatiotemporal signal detection in climate studies: A multiple-taper spectral domain approach, *Advances in Geophysics*, Vol. 41, Academic Press, 150 pp., 1999

[29] Yiou, P., M. F. Loutre, and E. Baert, "Spectral analysis of climate data", *Surv. Geophys.*, 17, 619–663, 1996.

[30] Mann M. E. and Lees J.M. , Mann, M. E., and J. M. Lees, "Robust estimation of background noise and signal detection in climatic time series", *Clim Change*, 33, 409–445, 1996.

[31] Ghil M, Allen RM, Dettinger MD, Ide K, Kondrashov D, Mann ME, Robertson A, Saunders A, Tian Y, Varadi F, Yiou P "Advanced spectral methods for climatic time series", *Rev Geophys*, 40(1),1–41, 2002.

[32] Elsner, J. B., and A. A. Tsonis, Singular Spectrum Analysis, A New Tool in Time Series Analysis, *Plenum Press*, New York, 1996.

[33] Vautard, R. et al., "Singular spectrum analysis, A toolkit for short noisy chaotic signals", *Phys.* D58, 95–126, 1992.

[34] Allen M, Smith L., "Monte Carlo SSA: Detecting irregular oscillations in the presence of colored noise*", J. Clim.* 9 (12):3373–3404, 1996.

[35] J. A. Schulte, C. Duffy, and R. G. Najjar, "Geometric and topological approaches to significance testing in wavelet analysis", *Nonlin. Processes Geophys. Discuss.* 1, 1331–1363, 2014

[36] Torrence C. and Compo G. P., "A Pratical Guide to Wavelet Analysis", *Bull. Am. Meteorolog. Soc.*, Vol.79 (1), 61-78, 1998.

[37] Grinsted A., Moore J. and Jevrejeva S., "Application of the cross wavelet transform and wavelet coherence to geophysical time series", *Nonlinear Process. Geophys.*, Vol. 11, 561-564, 2004.

[38] Jevrejeva, S., Moore, J. C., and Grinsted, A.: "Influence of the Arctic Oscillation and El Nino-Southern Oscillation (ENSO) on ice conditions in the Baltic Sea: The wavelet approach", *J. Geophys. Res.,* 108(D21), 4677, doi: 10.1029/2003JD003417, 2003.

[39] Velasco, V. M. and Mendoza B. "Assessing the relationship between solar activity and some large scale climatic phenomena", *Adv. Space Res*., 42, 866–878, 2008.

[40] Torrence, C. and Webster, P. , "Interdecadal changes in the ENSO-monsoon system", *J. Climate*", 1999, 12, 2679-2690

[41] D. Maraun and J. Kurths, "Nonstationary Gaussian processes in wavelet domain: Synthesis, estimation, and significance testing", *Phys. Rev. E* 75, 016707(2007)

[42] Nicholson E.S. and Dzefuli A.K., "The relationship rainfall variability in western equatorial Africa to the tropical oceans and atmospheric circulation. Part I: The boreal spring", *J. Climate*., Vol.26, 45-65, 2012.

[43] Dzefuli A.K. and Nicholson E.S., "The relationship rainfall variability in western equatorial Africa to the tropical oceans and atmospheric circulation". Part II: The boreal autumn", *J. Climate*., Vol. 26, 66-84, 2012.

[44] A. Farnsworth, E. White, Charles J.R. Williams, E. Black, and Dominic R. Kniveton**, "**Understanding the large scale driving mechanisms of rainfall variability over Central Africa"**,** *Advances in global change research* , Vol.3, 101-122, 2011.

[45] Wang C., S.-K. Lee and D. B. Enfield, "Atlantic Warm Pool acting as a link between Atlantic Multidecadal Oscillation and Atlantic tropical cyclone activity", *Geochem. Geophys. Geosyst.*, 9, Q05V03, doi:10.1029/2007GC001809, 2008.

[46] S. L. Hession and N. Moore, "A spatial regression analysis of the influence of topography on monthly rainfall in East Africa", *Int. J. Climatol*. 31, 1440–1456, 2011.

[47] P. Oettli and P. Camberlin, "Influence of topography on monthly rainfall distribution over East Africa", *Clim Res*, Vol. 28, 199–212, 2005.

[48] Xie S.P. and Carton, J. A., "Tropical Atlantic variability: Patterns, mechanisms, and impacts", *Earth's Climate*, Wiley Online Library, 121-142, 2004.